Xiang Ji[1]
Teng Zhou[1]
Yongbo Deng[2]
Liuyong Shi[1]
Xianman Zhang[1]
Sang Woo Joo[3]

[1]Mechanical and Electrical Engineering College, Hainan University, Haikou, Hainan, P. R. China
[2]Changchun Institute of Optics, Fine Mechanics and Physics (CIOMP), Chinese Academy of Science, Changchun, Jilin, P. R. China
[3]School of Mechanical Engineering, Yeungnam University, Gyongsan, South Korea

Received March 15, 2019
Revised May 17, 2019
Accepted May 31, 2019

Short Communication

A new droplet breakup phenomenon in electrokinetic flow through a microchannel constriction

A completely new droplet breakup phenomenon is reported for droplets passing through a constriction in an electrokinetic flow. The breakup occurs during the droplet shape recovery process past the constriction throat by the interplay of the dielectrophoretic stress release and the interface energy for droplets with smaller permittivity than that of the ambient fluid. There are conditions for constriction ratios and droplet size that the droplet breakup occurs. The numerical predictions provided here require experimental verification, and then can give rise to a novel microfluidic device design with novel droplet manipulations.

Keywords:
Dielectrophoresis / Droplet breakup / Microchannel constriction / Microfluidics / MST method
DOI 10.1002/elps.201900140

The need for precise droplet manipulation in microchannel flows arises frequently in many microfluidic devices and operations [1–4]. Advanced technologies have been developed for the control of small droplets, including those implementing dielectrophoresis (DEP) as vital means [5–8]. Many microchannels with different geometries have been investigated for the manipulation of different droplets or biological particles [9–14]. The converging-diverging geometry, or the microchannel constriction, is a generic configuration ubiquitous in microfluidic applications, and has been a subject of many investigations on DEP motion of droplets [15–21]. Under a variety of conditions, droplets can deform as they pass through the constriction to overcome adverse forces, including the negative DEP force blocking droplet migration into the constriction. Upon exiting the constriction, droplets would usually start to recover their shapes in the absence of any non-Newtonian effects. Here, we report a striking unexpected phenomenon of droplet breakup taking place instead of the shape recovery at the constriction downstream. There are existing studies on microfluidic droplet breakup, such as the splitting of confined droplets at microfluidic T-junctions [15, 22]. Spontaneous droplet breakup in electrokinetic flows without any external mechanical impact on the droplet, however, is a completely new phenomenon that requires careful considerations. In the present communication, we provide a first-time prediction on this phenomenon expecting more rigorous analyses and experimental investigations to follow.

A mathematical model of nonlinearly coupled electric, flow, and phase field is studied to investigate the electrokinetic droplet motion through a converging-diverging micro-channel, as shown in Fig. 1. The phase-field method is employed to track the interface between the droplet and the continuous phase (e.g. oil and water). The constriction channel geometry will give rise to non-uniform electric field and, in turn, the DEP force, which is calculated by using the Maxwell stress tensor (MST) method in this study [23–25].

The micro-channel can be divided into three parts, uniform inlet section, constriction section, and uniform outlet section. In the middle of constriction section is the throat, which coincides with the origin of 2D Cartesian coordinate system (x, y) used. The widths of inlet/outlet section and throat part are marked as w and b, and the quantities $w^* = \frac{w}{b}$ and $a^* = \frac{r}{b}$ are employed to represent the relative dimension of the throat and oil droplet.

The distribution of electric potential obeys the Laplace equation, as:

$$\nabla^2\phi = 0. \tag{1}$$

The electric field $\mathbf{E}$ obeys the equation as following:

$$\mathbf{E} = -\nabla\phi. \tag{2}$$

The boundary conditions for the electric field on the channel walls are

$$\phi = \phi_0 \text{ on } \mathrm{AB}, \tag{3}$$

Correspondence: Dr. Teng Zhou, Mechanical and Electrical Engineering College, Hainan University, Haikou 570228, Hainan, P. R. China
E-mail: zhouteng@hainu.edu.cn
Professor Sang Woo Joo, School of Mechanical Engineering, Yeungnam University, Gyongsan, South Korea
E-mail: swjoo@yu.ac.kr

Abbreviation: DEP, Dielectrophoresis; **MST**, Maxwell stress tensor

Color online: See the article online to view Figs. 1–3 in color.

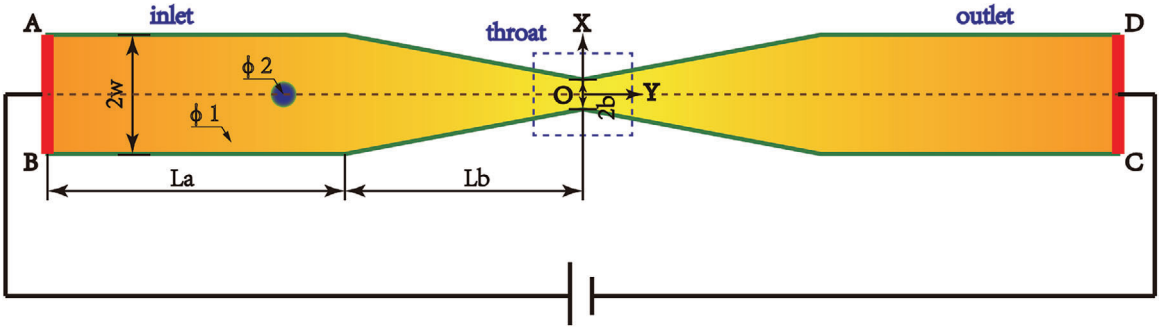

Figure 1. An oil droplet ϕ_2 is placed in water ϕ_1 which is confined to a converging-diverging structure. The quantities 2w and 2b represent the width of micro-channel and throat, respectively. The constant DC electric potentials are applied on the boundaries AB and CD.

$$\phi = 0 \quad \text{on CD.} \tag{4}$$

Other parts of the channel wall are electrically insulating.

The governing equations for the fluid motion are represented by the conservation of momentum and mass:

$$\rho \frac{\partial \mathbf{u}}{\partial t} + \rho\,(\mathbf{u}\cdot\nabla)\,\mathbf{u} = \nabla\cdot\left[-p\mathbf{I} + \mu\left(\nabla\mathbf{u} + \nabla\mathbf{u}^T\right)\right] + \mathbf{F}_{st} + \rho\mathbf{g} + \mathbf{F}, \tag{5}$$

$$\nabla\cdot\mathbf{u} = 0. \tag{6}$$

Here, ρ and μ represent the density and dynamic viscosity of water phase or oil phase, and the quantities $\mathbf{F}_{st}$, $\rho\mathbf{g}$, and $\mathbf{F}$ represent the surface tension force, gravity force, and electric force, respectively.

The electric force $\mathbf{F}$ is defined as additional volume force, and the electric force is given by the divergence of the MST:

$$\mathbf{F} = \nabla\cdot\mathbf{T}. \tag{7}$$

The MST follows the equation:

$$\mathbf{T} = \mathbf{E}\mathbf{D}^T - \frac{1}{2}(\mathbf{E}\cdot\mathbf{D})\mathbf{I}, \tag{8}$$

where $\mathbf{E}$ is the electric field intensity and $\mathbf{D} = \varepsilon_0\varepsilon_w\mathbf{E}$ is the electric displacement field, ε_w is the permittivity of water.

To track the fluid interface, the laminar two-phase flow, phase field interface uses a phase field method:

$$\frac{\partial\lambda}{\partial t} + \mathbf{u}\cdot\nabla\lambda = \nabla\cdot\frac{3\chi\delta\varepsilon_w}{2\sqrt{2}}\nabla\psi, \tag{9}$$

$$\psi = -\nabla\cdot{\varepsilon_w}^2\nabla\lambda + \left(\lambda^2 - 1\right)\lambda. \tag{10}$$

The phase field variable λ is -1 in water and 1 in oil, δ is the surface tension coefficient, the quantity $\varepsilon = 0.05r_d$ is a numerical parameter which determines the thickness between the oil droplet phase and water phase, and the quantity $\chi = 1$ controls the mobility of the interface.

As Fig. 2 shows, the splitting phenomenon of oil droplets in converging-diverging microchannels is investigated in this paper, and the splitting process can be divided as four stages. The density and dynamic viscosity of oil droplet λ_2 are set as 884 kg/m^3 and 0.474 kg/m s, and the carrier fluid

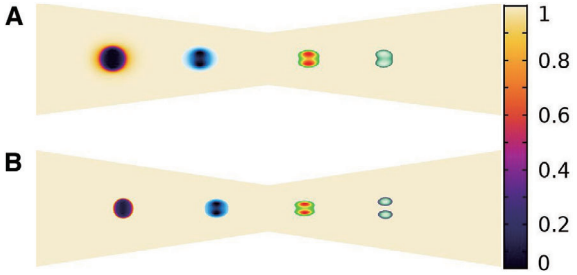

Figure 2. The splitting process of an oil droplet initially located at (x, y) = (0.5 Lb, 0) with the radius ratio $a^* = 0.5$; (A) and (B) represent the transport process of an oil droplet with the contraction ratios $w^* = 2.9$ and $w^* = 3.2$, respectively.

λ_1 is water. The permittivity of oil and water is 2.2 and 80.2, respectively. An electric potential $V_0 = 50$ V is applied on the relative electrical boundaries. The lengths of microchannels are $L_a = 500$ μm and $L_b = 400$ μm, respectively.

Figure 3 describes the effects of parameters associated with droplet motion and channel structure on the droplet breakup. Velocity along the centerline of the channel is monitored until the droplet ceases to advance streamwise and begins to split and migrate spanwise. As Fig. 3A shows, in converging region the droplets in the channel with constriction ratio $w^* = 2.9$ and $w^* = 3.2$ show increase in streamwise velocity. Past the throat, however, the droplet in the channel with the higher constriction ratio $w^* = 3.2$ splits into two identical droplets, with the centerline streamwise velocity diminishing to zero.

The splitting phenomenon of two liquid phases is generally attributed to the changes in surface tension, so the numerical simulation neglecting the surface tension coefficient is performed. As Fig. 3B shows, the x-component velocities of oil droplets vary with time, and in this section, the droplets are suspended in the channel with contraction ratio $w^* = 3.2$, however, the surface tension coefficient is neglected, so the droplet passes through the throat without splitting.

The droplet breakup often arises from the change in geometrical conditions, so the constriction ratio w^* and radius ratio a^* are employed as main parameters in investigating the breakup conditions. As Fig. 3C shows, for droplets with a fixed radius ratio a^*, higher constriction ratio w^* facilitates

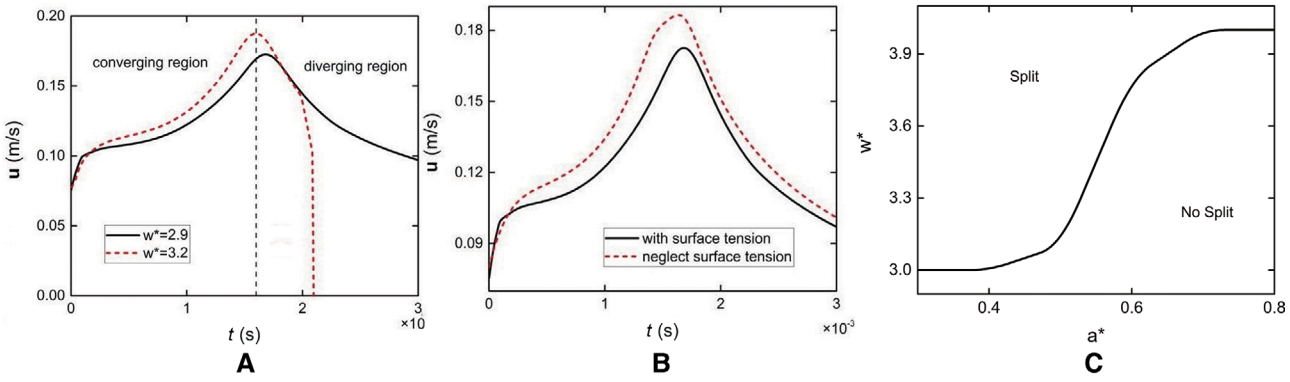

Figure 3. The x-component velocities (A), (B) and splitting region (C) of oil droplets with different radius ratios a^* and contraction ratios w^*; (B) represents the comparison of oil droplets transport with or without surface tension in phase fields.

the droplet breakup, while for a fixed constriction ratio w^*, the breakup region expands with the radius ratio a^*. Based on this fundamental principle, various micro-devices can be designed to utilize the droplets splitting.

The breakup phenomenon of oil droplets in converging-diverging microchannels is numerically studied by the phase field method, with the MST method for the calculation of the DEP force. The simulation results show that depending on the constriction ratio and the droplet size, an oil droplet either can pass through the constriction completely or breakup into two parts. For the laterally symmetric geometry and flow conditions studied here, the breakup always results in two identical drops. Asymmetric conditions may initiate an asymmetric breakup, which needs to be verified through further studies. This numerical study also requires experimental verification that can eventually provide a design range of the microchannel structures for new DEP droplet control.

This work is funded by National Natural Science Foundation of China (Grant No. 51605124), Scientific Research Foundation of Hainan University (Grant No. Kyqd1569,hdkyxj201721, and hdkyxj201722), and the National Research Foundation of Korea (Grant NRF-2018R1A2B3001246).

The authors have declared no conflict of interest.

References

[1] Barbulovic-Nad, I., Xuan, X., Lee, J. S., Li, D., *Lab Chip* 2006, *6*, 274–279.

[2] Kaminski, T. S., Scheler, O., Garstecki, P., *Lab Chip* 2016, *16*, 2168–2187.

[3] Li, M., Li, D., *J. Chromatogr. A* 2017, *1501*, 151–160.

[4] Si, T., Yin, C., Gao, P., Li, G., Ding, H., He, X., Xie, B., Xu, R. X., *Appl. Phys. Lett.* 2016, *108*, 021601.

[5] Yang, S. M., Yao, H., Zhang, D., Li, W. J., Kung, H. F., Chen, S. C., *Microfluid. Nanofluid.* 2015, *19*, 235-243.

[6] Jung-Yeul, J., Ho-Young, K., *Anal. Chem.* 2007, *79*, 5087.

[7] Li, S., Ren, Y., Cui, H., Yuan, Q., Wu, J., Eda, S., Jiang, H., *Electrophoresis* 2015, *36*, 471–474.

[8] Demisch, L., *Phys. Rev. Lett.* 2004, *92*, 054503.

[9] Liang, L., Ai, Y., Zhu, J., Qian, S., Xuan, X., *J. Colloid Interface Sci.* 2010, *347*, 142–146.

[10] Dubose, J., Lu, X., Patel, S., Qian, S., Woo Joo, S., Xuan, X., *Biomicrofluidics* 2014, *8*, 014101.

[11] Zhu, J., Xuan, X., *J. Colloid Interface Sci.* 2009, *340*, 285–290.

[12] Zhu, J., Tzeng, T.-R. J., Hu, G., Xuan, X., *Microfluid. Nanofluid.* 2009, *7*, 751–756.

[13] Ai, Y., Park, S., Zhu, J., Xuan, X., Beskok, A., Qian, S., *Langmuir* 2010, *26*, 2937–2944.

[14] Sinz, D. K., Darhuber, A. A., *Lab Chip* 2012, *12*, 705–707.

[15] Lu, X., Patel, S., Zhang, M., Woo Joo, S., Qian, S., Ogale, A., Xuan, X., *Biomicrofluidics* 2014, *8*, 021802.

[16] Sharma, S., Srisa-Art, M., Scott, S., Asthana, A., Cass, A., *Methods Mol. Biol.* 2013, *949*, 207.

[17] Yang, Y. J., Feng, X., Xu, N., Pang, D. W., Zhang, Z. L., *Appl. Phys. Lett.* 2013, *102*, 14613–14619.

[18] Zhou, T., Ge, J., Shi, L., Fan, J., Liu, Z., Woo, J. S., *Electrophoresis* 2018, *39*, 590.

[19] Ai, Y., Qian, S., Liu, S., Joo, S. W., *Biomicrofluidics* 2010, *4*, 013201.

[20] Ai, Y., Joo, S. W., Jiang, Y., Xuan, X., Qian, S., *Electrophoresis* 2009, *30*, 2499–2506.

[21] Zhou, T., Ji, X., Shi, L., Zhang, X., Deng, Y., Joo, S. W., *Electrophoresis* 2019, *40*, 993–999.

[22] Christopher, G. F., Bergstein, J., End, N. B., Poon, M., Nguyen, C., Anna, S. L., *Lab Chip* 2009, *9*, 1102–1109.

[23] Zhou, T., Deng, Y., Zhao, H., Zhang, X., Shi, L., Woo Joo, S., *J. Fluids Eng.* 2018, *140*, 091302.

[24] Ai, Y., Qian, S., *J. Colloid Interface Sci.* 2010, *346*, 448–454.

[25] Ai, Y., Zeng, Z., Qian, S., *J. Colloid Interface Sci.* 2014, *417*, 72–79.

